Bull. Mater. Sci., Vol. 37, No. 3, May 2014, pp. 519–525. © Indian Academy of Sciences.

# Microstructural and optical properties of transparent conductive ZnO : Al : Mo films deposited by template-assisted sol–gel method

**H -Y HE*, J -F HUANG, Z HE, J LU and Q SHEN**

College of Materials Science and Engineering, Shaanxi University of Science and Technology, China 710021

MS received 11 November 2012; revised 22 January 2013

**Abstract. Transparent conductive ZnO : Al : Mo films with a molar ratio of Zn : Al : Mo = 99 : 0·99 : 0·01 were deposited on quartz glass substrate by a template-assisted sol-gel process and characterized by X-ray diffraction, atomic force microscopy, scanning electron microscopy, and UV–Vis and luminescent spectrophotometries. The four types of organic template have induced nanowire morphology with varying aspect ratio. Dip coating in one constant positive and reverse direction causes the parallel array of ZnO : Al : Mo nanowires on the quartz glass substrate. Long and parallel arrayed nanowire films show obviously blue shifts and enhanced transmittances in the UV-Vis light range. The PEG-1000 and PEG-2000 have optimal effects among four templates as constant weight content is used. The films show strong ultraviolet, violet and bluish violet emissions. The templates also lead to overall thicker film and more native defect and thereby remarkably enhancing photoluminescence of the films. Long chain organic template can be used to optimize the optical properties of the doped ZnO film.**

**Keywords. ZnO; nanowire; array; transmittance; blue shift; photoluminescence.**

## 1. Introduction

Transparent conducting thin film made of aluminum-doped zinc oxide (AZO) has attracted wide attentions because of its superiority over indium doped tin oxide (ITO) used as transparent conducting film in the optical electronic industries, including solar cells, gas sensors, piezoelectric transducers and varistors (Gupta and Mansingh 1996; Polla *et al* 1996; Beeke *et al* 2006; Wang and Song 2006; Wang *et al* 2007; Liu *et al* 2007). Zinc oxide (ZnO) is a wide bandgap II–VI semiconductor (3·2–3·37 eV) with very attractive properties, including high transparency in the visible wavelength, a high piezoelectric constant, a large electro-optic coefficient (Bertolotti *et al* 1990) and a large exciton binding energy (~ 60 meV) at room temperature. It is non-toxic, inexpensive, and found in rich reserve in the earth crust of Zn and O elements.

To improve the electrical and optical properties of ZnO films, some dopants, such as Al, Si, In and Ga are often used (Hirata *et al* 1996; Reddy and Miles 1998; Nunes *et al* 1999). Al-doped ZnO (AZO), especially, has shown good electrical and optical properties. Moreover, the widening in bandgap of the ZnO induced by Ti-, Ca-, Si, Sc and Mo-dopants has recently been reported (Lin *et al* 2000; Tadatsugu *et al* 2000; Lin *et al* 2005; Das *et al* 2009; Misra *et al* 2009; Wu *et al* 2009). This widening in the bandgap is generally attributed to the known Moss–Burstein shift. Moreover, (Al, Sc)-codoping into the ZnO film can lead to better electric conductivity, higher transmittance and wider bandgap than the Al-doping and Sc-doping at an appropriate amount of Sc proportion (Lin *et al* 2008a, b; Chen *et al* 2009). In our previous studies, appropriate amount of Mo, W, or Si-codoping also led to the bandgap broadening and the transmittance enhancement of the Al-doped ZnO nanocrystalline powders (He and Guo 2011; He and Liang 2012a, b). Furthermore, it is well known that one dimensional nanostructure and their reasonable array can result in improvement in some properties of the materials. In this paper, we report the organic template effects on the microstructure and optical properties of the ZnO : Al : Mo films deposited by sol–gel process.

## 2. Material and methods

0·01 mole $Zn(NO_3)_2{\cdot}6H_2O$ was dissolved in 50 mL ethanol in a glass beaker, and then approximate amounts of triethanolamine (5 mL) and glycol ethanol (5 mL) were added to stabilize the solutions. To enhance the accuracy of weighing, $Al(NO_3)_3{\cdot}9H_2O$ and $(NH_4)_6Mo_7O_{24}{\cdot}4H_2O$ at a molar ratio of Mo : Al = 0·01 were separately dissolved in 100 mL ethanol in other two glass beakers. The solutions containing Al and Mo cations were taken by volume and then added to the solution containing Zn cation at molar ratio of Zn : Al : Mo = 99 : 0·99 : 0·01. A small

*Author for correspondence (hehy@sust.edu.cn)

amount of hydrochloric acid (~ 0·5 mL) was added to prevent the formation of hydroxide. The volume of the solution was expanded to 100 mL by adding ethanol, so that the molar concentration of the $Zn^{2+}$ cation reached 0·1 mol $L^{-1}$. Into each one of such four solutions, 2 g PEG-1000, PEG-2000, PEG-4000, and PVP (k30) as templates were then added, respectively. After an ageing of several hours at room temperature, the solutions with and without template were dip coated on quartz glass substrates with length of 25 mm and width of 25 mm and thickness of 1 mm. The pulling film from the solution was controlled in alternately positive and reverse directions and at a speed of ~ 10 cm $min^{-1}$ and a static setting at slantwise angle of ~ 45° for waiting other film coatings. After each coating, the film was dried at 120–150 °C for 2–4 min. The ten layer films were obtained by repeating dip coating and drying. The as-deposited films were finally annealed at 600 °C for 60 min.

The phase and structure of the deposited ZnO : Al : Mo films were identified at room temperature using an X-ray diffractometer (XRD, $CuK_{\alpha 1}$, $\lambda = 0{\cdot}15406$ nm, Model No: D/Max-2200PC, Rigaku, Japan). The texture, particle size, and thickness of the films were analyzed using atomic force microscopy (AFM, Model No: SPI3800N, Japan) and scanning electron microscope (SEM, Model No: S-4800, Hitachi, Japan). The light transmittance and reflectance of the films were determined with UV–Vis spectrophotometer (Model No: 752N, China) in wavelength range of 300–860 nm. The photoluminescence spectra of the films was recorded on a luminescent spectrophotometer (Model no. F-4600, Hitachi, Japan).

## 3. Results and discussion

Figure 1 shows the XRD patterns of the ZnO : Al : Mo films. The wurtzite ZnO is the only XRD detectable phase of the films (PDF#36-1451). This might indicate that the $Al^{3+}$ and $Mo^{6+}$ cations enter the ZnO lattice by cation substitution. Low XRD peaks could be due to smaller film thickness.

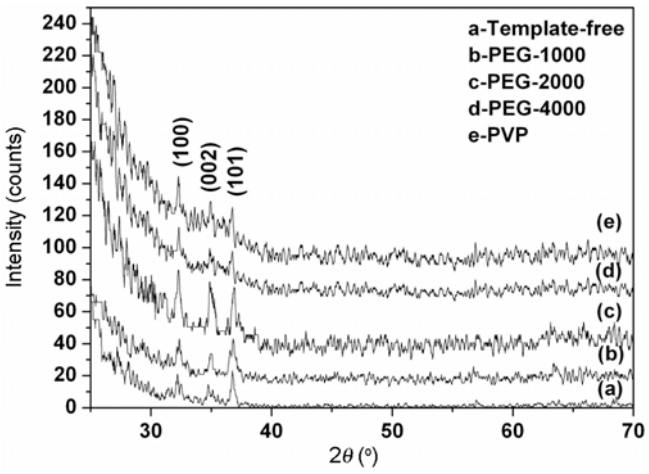


**Figure 1.** XRD patterns of ZnO : Al : Mo films deposited with and without template.

Figure 2 shows AFM micrographs of the ZnO : Al : Mo films. The film deposited without template shows uniform and randomly oriented spherical morphology with average particle size of ~ 75 nm (figure 2a). The film deposited with PEG-1000 shows a nanowire morphology with an average size of ~ 9 nm in width and 90 nm in length (figure 2b), while the films deposited with and PEG-2000 similarly shows a longer and thinner parallel nanowire morphology with an average size of ~ 5 nm in width and 130 nm in length (figure 2c). However, the PEG-4000 and PVP lead to longer but wider nanowire morphologies (figures 2d and e), respectively. It also can be seen from figures 2(b–e) that the nanowires are running parallel with each other and to growth plane. Real array may not be so regular, but some of them are certainly running parallel to or approximately parallel to growth plane. The formation of the different morphologies could be mainly ascribed to the inductive effect of the long-chain templates and the dip coating in constant positive and opposite direction. PEG-4000 and PVP have longer molecular chain but smaller number of molecules limited by the constant addition of 2 g, and thereby causing longer but wider nanowires. In addition, too long PEG-4000 and PVP molecular chain cannot be easily stretched in the process of dip coating, which could be another reason for their induced nanowire morphology.

Figure 3 shows the cross-section SEM micrographs of the ZnO : Al : Mo films. The thickness of the films is estimated to be ~ 2·8, ~ 3·8, ~ 2·5, ~ 2·4 and ~ 8·5 $\mu$m for the template-free, PEG-1000, PEG-2000, PEG-4000, and PVP, respectively. Only PEG 1000 and PVP templates give larger film thicknesses than template-free. The difference in thickness could come from the difference in viscosity of the precursor solution resulting from the templates and some difference in speed of the dip coating. Furthermore, figures 3(b–e) demonstrate the nanowires are parallel to growth plane to some extent, which confirms the results observed from AFM micrographs.

Figure 4 shows the transmittance and reflectance spectra of the ZnO : Al : Mo films deposited with and without template. The visible light transmittance is ~ 80–90% as template-free and using PEG, and ~ 60% as using PVP (table 1). The films deposited with PEG1000 and PVP have larger film thickness and thereby exhibiting relatively smaller transmittances. Moreover, the light transmissions of the films blue shift to violet-light region below 350 nm to different degrees. Differences among the blue shifts and transmittances of the films could be mainly ascribed to their differences in thickness, anisotropy growth and array.

Wurtzite structure ZnO has a direct bandgap, so that the optical bandgap ($E_g$) of the films can be calculated

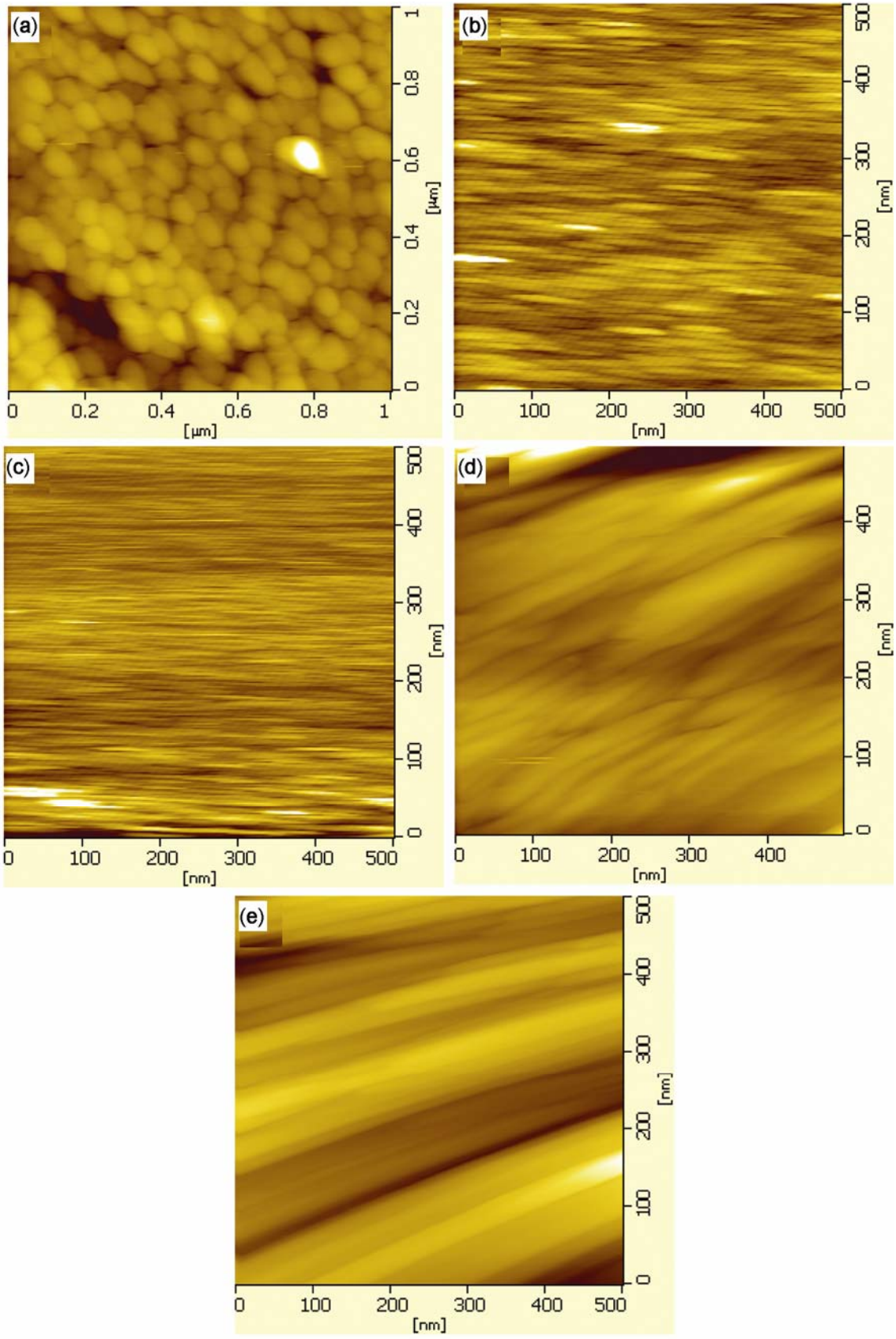


**Figure 2.** AFM micrographs of ZnO : Al : Mo films deposited (**a**) without and with template, (**b**) PEG-1000, (**c**) PEG-2000, (**d**) PEG-4000 and (**e**) PVP.

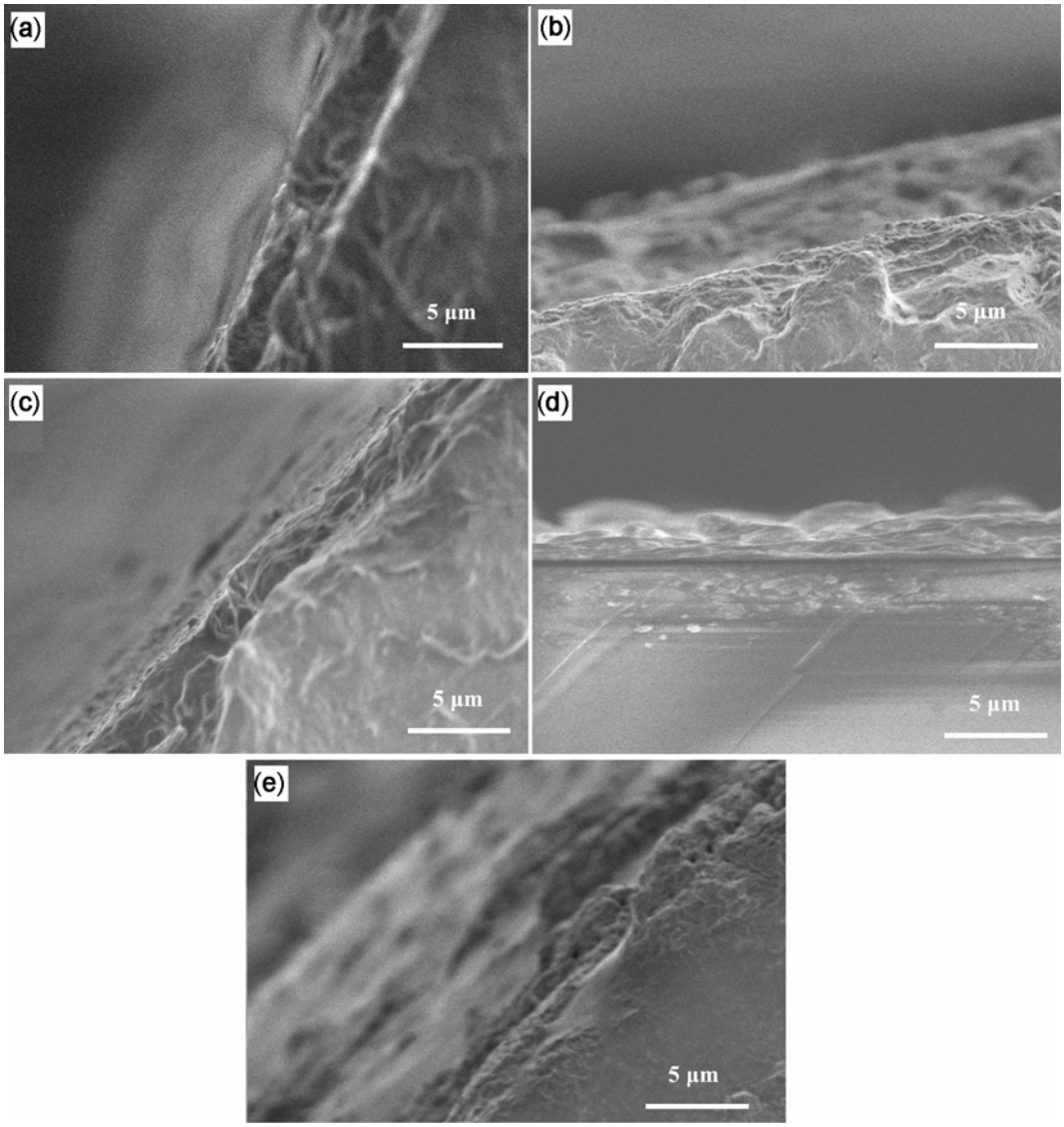


**Figure 3.** Cross-section SEM micrographs of ZnO : Al : Mo films deposited (**a**) without and with template, (**b**) PEG-1000, (**c**) PEG-2000, (**d**) PEG-4000 and (**e**) PVP.

with the following relationship (Pankove *et al* 1975; Serpone 1995):

$$(\alpha h\nu)^2 = \mathrm{C}(h\nu - E_g), \tag{1}$$

where $h\nu$ is photon energy and $C$ is a constant, and $\alpha$ is absorption coefficient (Pankove *et al* 1975):

$$\alpha = \frac{1}{d}\left(\ln\frac{1-R}{T}\right), \tag{2}$$

where $T$ is the transmittance and $d$ the film thickness. $R$ is reflectance. Figure 5 shows graphs of $(\alpha h\nu)^2$ vs photon energy $h\nu$ for the ZnO : Al : Mo thin films. The linear dependence of $(\alpha h\nu)^2$ on $h\nu$ at higher photon energies indicates that the ZnO : Al : Mo films are essentially direct–transition-type semiconductors. The straight-line portion of the curve, when extrapolated to zero, gives the optical bandgap $E_g$ (table 1). The constant $C$ was calculated from the reciprocal gradient of the linear portion in these curves. The calculated $C$ values are also listed in table 1. From the results of figure 5, $E_g$ is in a range of 3·29–3·54 eV. These values are overall larger than 3·2–3·37 eV of pure ZnO. The widening in the bandgap with respect to pure ZnO, which is the known Moss–Burstein shift, resulted from (Al, Mo)-co-substitution in the nanofilms (Lin *et al* 2008a, b; Chen *et al* 2009; He and Liang 2012a; He *et al* 2012b; He and Guo 2011). If the bandgap of pure bulk ZnO is 3·2 eV (Xu and Schoonen 2000), this Moss–Burstein shift should be 0·09 eV as ignoring size effect that narrows the bandgap. In Addition, a Moss–Burstein shift is estimated to be ~ 0·03 eV in sol–gel deposited Al-doped ZnO films when Al-doping amount is

1% (Wang *et al* 2009), and is ~ 0·024 eV in $Zn_{0.99}Al_{0.01}O$ powders due to Mo-codoping at molar ratio of Mo/Al = 0·01 (He and Liang 2012a). Accordingly, the Moss–Burstein shift that resulted from the (Al, Mo)-codoping could be ~ 0·054 eV. The films deposited with four types of templates show further blue shifts, in which PEG-1000 and PEG-2000 have optimal effect. The widening of bandgap induced by templates could majorly come from the template-induced anisotropy growth and parallel array of the nanowires. The crystal anisotropy can lead to the optical anisotropy and thereby leading to the enhanced and blue shifted light transmission of the film. This phenomenon has been reported in previous literatures (Wraback *et al* 1999; Schaadt *et al* 2007; Lin *et al* 2009). That is, the *c*-oriented and parallel arrayed film has greater polarized optical transmittance and blue shift in direction parallel to the *c*-axis compared with that in direction perpendicular to the *c*-axis. This could imply that the polarized optical transmittance and blue shift in direction parallel to the *c*-axis increase with increase in the aspect ratio of the nanowires. The larger the aspect ratio of the nanowires, the greater the transmittance difference and larger the blue shift of the film. Gorla *et al* (1999) attributed this phenomenon to the anisotropy in absorption associated with the polarization selection rules and the effect of a thermally induced in-plane anisotropic strain, combined with the separation in energy of the *C* band from the *A* and *B* bands of ZnO.

Figures 6 and 7 illustrate the photoluminescence spectra of ZnO : Al : Mo films. They were measured at monitoring wavelength $\lambda_{em}$ = 410 nm (~ 3·02 eV) and exciting wavelength $\lambda_{ex}$ = 325 nm (~ 3·82 eV). The excitation peaks of the films deposited with template-free, PEG-1000, PEG-2000, PEG-4000, and PVP are centred at ~ 381·2 nm (~ 3·25 eV), ~ 369·4 nm (~ 3·36 eV), ~ 367·2 nm (~ 3·38 eV), ~ 379·5 nm (~ 3·27 eV), ~ 367·8 nm (~ 3·37 eV), respectively. They could be ascribed to near bandgap absorption, and shift conformably with the variations of the bandgap estimated from the transmittance spectra. The emission peaks are centred at ~ 391 nm (~ 3·17 eV), ~ 410 nm (~ 3·02 eV) and ~ 433 nm (~ 2·86 eV) for all films. The emissions centred at ~ 391 nm could be near

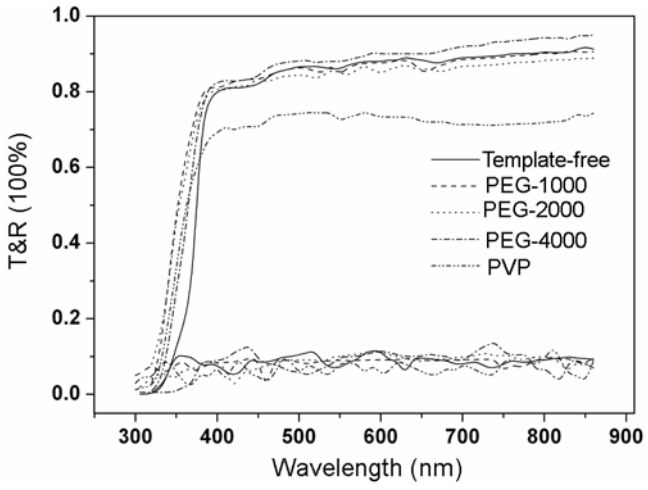


**Figure 4.** Transmittance and reflectance spectra of ZnO : Al : Mo films deposited with and without template.

**Table 1.** Thickness ($d$), average transmittance ($T_a$), bandgap energy ($E_g$) and constant C of the ZnO : Al : Mo films.

| Sample | $d$ ($\mu$m) | $T_a$ (100%) | $E_g$ (eV) | C ($10^{12}$ eV·m$^{-2}$) |
|---|---|---|---|---|
| Template-free | 48 | 67·5 | 3·34 | 2·89 |
| PEG-1000 | 153 | 67·6 | 3·51 | 1·88 |
| PEG-2000 | 49 | 74·9 | 3·48 | 2·19 |
| PEG-4000 | 25 | 68·4 | 3·47 | 8·60 |
| PVP | 50 | 65·5 | 3·43 | 3·17 |

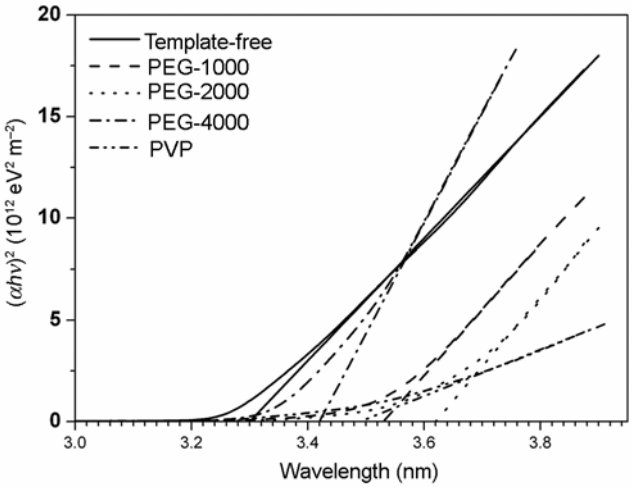


**Figure 5.** Plots of $(\alpha h\nu)^2$ vs $h\nu$ for ZnO : Al : Mo films deposited with and without template.

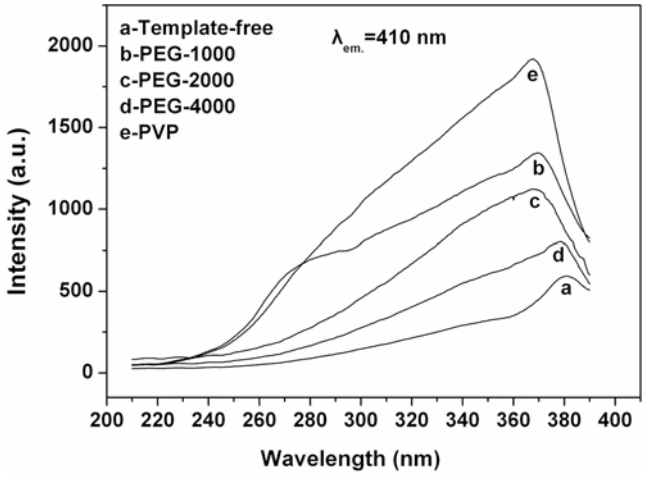


**Figure 6.** Excitation spectra of ZnO : Al : Mo films deposited with and without template.

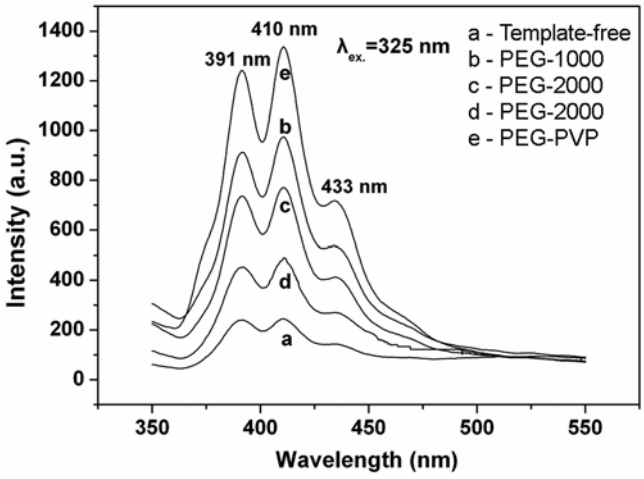


**Figure 7.** Emission spectra of ZnO : Al : Mo films deposited with and without template.

bandgap emission (Ma and Wang 2012) or related to bandgap (Ekthammathat *et al* 2012), The strong band centred at 410 nm and weak band centred at 433 nm correspond to a violet emission and a bluish violet emission, respectively. The ZnO material usually exhibits visible emissions that are generally attributed to native defects, including surface defects, interstitial defects, and the adsorption of impurities on the surfaces of the ZnO matertials [oxygen vacancy (VO), zinc vacancy (VZn), oxygen interstitial (Oi), zinc interstitial (Zni) and antisite oxygen (OZn)] in ZnO (Rakhesh *et al* 2007; Ekthammathat *et al* 2012; Ma and Wang 2012). The energy levels of intrinsic defects in ZnO film have been calculated using full-potential linear muffin-tin orbital method in literature (Sun 2000; Lin *et al* 2001). According to the calculation, the energy interval from the bottom of the conduction band to the Zn vacancy (VZn) level is ~3·06 eV. This electron transition has been used to interpret the emissions centred at 401 nm (~3·09 eV) and 400 nm (~3·1 eV) in literature (Jeong *et al* 2003; Gu *et al* 2012). Therefore, the violet emission peak at 410 nm (~3·03 eV) in this study can be ascribed to the electron transition from the bottom of the conduction band to the Zn vacancy levels. Similarly, the energy interval from the top of the valence band to the zinc interstitial (Zni) level equals to ~2·9 eV (Sun 2000) and thereby being responsible for the bluish violet emission centred at ~433 nm (~2·86 eV) in this study. Accordingly, the native defect in the films deposited in this work is mainly the Zn vacancy (VZn) and smaller amounts of zinc interstitial (Zni), which is conformable with the deposition conditions of low temperature and air oxidation atmosphere. In addition, the blue emissions centred at 451 nm (~2·75 eV) and 450 nm (~2·76 eV) near 2·9 eV are also ascribed to the presence of oxygen vacancies, respectively (Baibarac *et al* 2008; Gu *et al* 2012).

The photoluminescence, especially the emission, of the films deposited with and without templates exhibits very different intensity. It is well known that a thicker film is expected to have a stronger photoluminescence signal, the increase in the concentration of the native defect means an enhancement in photoluminescence originating from the defect, and larger specific surface area resulting from particle size and roughness and can possess larger content of surface defect and thereby causing stronger photoluminescence. Thus, the variations in intensities of the excitation and emission peaks can be ascribed to both the film thickness and utilization of the template that usually leads to high content of the native defect in the film. Moreover, the templates lead to obvious variations in the average particle size of the films. The films deposited with PEG-4000 and PVP especially have larger particle sizes but comparable emission intensity, even if the effects of film thicknesses have been taken into account. This indicates that the differences among defect contents in the films induced by different templates seem to be near or greater than the differences in contents of the surface defect that resulted from the particle size, and longer template molecular chain lead to larger concentration of the native defects. In addition, Chattopadhyay *et al* (2012) reveals that the increase of the disorder in the system can lead to a decrease in band edge emission in ZnO expecting the grain size. This phenomenon can also be observed from the slightly slower increase in intensity of the emission peak centred at 391 nm compared to that of the emission peak centred at 410 nm and 433 nm due to an increase in chain length of template molecule, which also implies that the concentration of the defect in the films increases with the chain length of the templates. Thus, the variations in the photoluminescence intensities are mainly dependent on the film thickness and defect concentration.

## 4. Conclusions

Transparent conductive ZnO : Al : Mo films with constant molar ratio of 99 : 0·99 : 0·01 had been synthesized by a template-assisted sol–gel method. The template had a significant effect on the average particle size, the morphology, the transmittance and the bandgap energy of the films. Using long-chain templates, the morphology is transferred to long nanowire, and the transmittance of the films in the range of UV-visible light is enhanced and blue-shifted. The PEG-1000 and PEG-2000 have optimal effect among the four templates as constant weight content is used. In addition, the templates result in overall thicker films and obvious increased native defect concentration in the films and thereby enhancing the emissions of the films in the range of UV-visible light at different degrees. The improvement in optical properties of the film by using the long-chain template may be of significance to

the application of various transparent conductive ZnO films.

**Acknowledgements**

The authors gratefully acknowledge the financial assistance provided by the Natural Scientific Fund Projects of Shaanxi Province (2012JM6008).

**References**

Baibarac M, Baltog I, Lefrant S, Mevellec J Y and Husanu M 2008 *Physica* **E40** 2556

Beeke W J, Wienk M M and Janssen R A J 2006 *Adv. Funct. Mater.* **16** 1112

Bertolotti M, Laschena M V, Rossi M, Ferrari A, Qian L S, Quaranta F and Valentini A 1990 *J. Mater. Res.* **5** 1929

Chattopadhyay S, Neogi S K, Pandit P, Dutta S, Rakshit T, Jana D, Chattopadhyay S, Sarkar A and Ray S K 2012 *J. Lumin.* **132** 6

Chen J L, Chen D, He J J, Zhang S Y and Chen Z H 2009 *Appl. Surf. Sci.* **255** 9413

Das A K, Misra P and Kukreja L M 2009 *J. Phys. D: Appl. Phys.* **42** 165405

Ekthammathat N, Thongtem T, Phuruangrat A and Thongtem S 2012 *Ceram. International*. (in press)

Gorla C R, Emanetoglu N W, Liang S, Mayo W E and Lu Y 1999 *J. Appl. Phys.* **85** 2595

Gu P F, Wang X D, Li T, Meng H M, Yu H Y and Fan Z H 2012 *J. Cryst. Growth* **338** 162

Gupta V and Mansingh A 1996 *J. Appl. Phys.* **80** 1063

He H Y and Guo J M 2011. *Micro. & Nano Letts.* **6** 725

He H Y and Liang Q 2012a *Curr. Appl. Phys.* **12** 865

He H -Y, He Z, Shen Q and Lu J 2012b *J. Mater. Sci.* (in press)

Hirata G A, Mekittrik J, Cheek T, Siqueiros J M, Diaz J A, Contreras O and Lopex O A 1996 *Thin Solid Films* **228** 29

Jeong S H, Kim B S and Lee B T 2003 *Appl. Phys. Lett.* **82** 2625

Lin B X, Fu Z X and Jia Y B 2001 *Appl. Phys. Lett.* **79** 943

Lin Su-Shi, Huang Jow-Lay and Sajgalik P 2005 *Surf. Coat. Tech.* **191** 286

Lin J C, Peng K C, Liao H -L and Lee S L 2008a *Thin Solid Films* **516** 5349

Lin J C, Peng K C, Tseng C A and Lee S L 2008b *Surf. Coat. Tech.* **202** 5480

Lin H, Zhou S M, Huang T H, Teng H, Liu X D, Gu S L, Zhu S M, Xie Z L, Han P and Zhang R 2009 *J. Alloys Compd.* **467** L8

Lin Y C, Wang B L, Yen W T, Ha C T and Peng Chris 2010 *Thin Solid Films* **518** 4928

Liu H Y, Kong H, Ma X M and Shi W Z 2007 *J. Mater. Sci.* **42** 2637

Ma X Y and Wang Z 2012 *Mater. Sci. Semicond. Process* **15** 227

Misra K P, Shukla R K, Srivastava A and Srivastava A 2009 *Appl. Phys. Lett.* **95** 031901

Nunes P, Fernandes B, Fortunan E, Vilarinlo P and Martins R 1999 *Thin Solid Films* **337** 176

Pankove J I 1975 *Optical processes in semiconductors* (New York: Dover)

Polla D L, Muller R S and White R M 1996 *IEEE Electron Device Lett.* **7** 254

Rakhesh V, Bushiri M J and Vaidyan V K 2007 *J. Optoelectron. Adv. Mater.* **9** 3740

Reddy K T R and Miles R W 1998 *J. Mater. Sci. Lett.* **17** 279

Schaadt D M, Brandt O, Ghosh S, Flissikowski T, Jahn U and Grahn H T 2007 *Appl. Phys. Lett.* **90** 231117

Serpone N, Lawless D and Khairutdinov R 1995 *J. Phys. Chem.* **99** 16646

Sun Y M 2000 Ph D thesis, University of Science and Technology of China

Tadatsugu Minami, Takashi Yamamoto and Toshihiro Miyata 2000 *Thin Solid Films* **366** 63

Wang Z L and Song J H 2006 *Science* **312** 242

Wang M -S, Lee K E, Hahn S H, Kim E J, Kim S, Chung J S, Shin E W and Park C 2007 *Mater. Lett.* **61** 1118

Wraback M, Shen H, Liang S, Gorla C R and Lu Y 1999 *Appl. Phys. Lett.* **74** 507

Wu C G, Shen J, Ma J, Wang S P, Zhang Z. G and Yang X L 2009 *Semicond. Sci. Technol.* **24** 125012

Xu Y and Schoonen M A A 2000 *American Mineralogist* **85** 543